Inorg. Chem. **2002**, *41*, 4389–4395

Excited-State Electronic Coupling and Photoinduced Multiple Electron Transfer in Two Related Ligand-Bridged Hexanuclear Mixed-Valence Compounds

Brian W. Pfennig,* Carolyn J. Mordas, Alex McCloskey, Jenny V. Lockard, Patty M. Salmon, Jamie L. Cohen, David F. Watson, and Andrew B. Bocarsly

Department of Chemistry, Princeton University, Washington Road, Princeton, New Jersey 08544

Received March 25, 2002

The synthesis, characterization, electrochemical, photophysical, and photochemical properties of two hexanuclear mixed-valence compounds are reported. Each supramolecular species consists of two cyano-bridged $[(NC)_5Fe^{II}$-CN-$Pt^{IV}(NH_3)_3$L-NC-$Fe^{II}(CN)_5]$ triads that are linked to each other through a Pt^{IV}-L-Pt^{IV} bridge, where L = 4,4′-dipyridyl (bpy) or 3,3′-dimethyl-4,4′-dipyridyl (dmb). The major difference between the two compounds is the electronic nature of the bridging ligand between the two Pt atoms. Both species exhibit a broad Fe(II) → Pt(IV) intervalent (IT) absorption band at 421 nm with an oscillator strength that is approximately four times that for $[(NC)_5Fe^{II}$-CN-$Pt^{IV}(NH_3)_5]$ and twice that for $[(NC)_5Fe^{II}$-CN-$Pt^{IV}(NH_3)_4$-NC-$Fe^{II}(CN)_5]^{4-}$. When L = bpy, the resonance Raman spectrum obtained by irradiating the IT band at 488 nm exhibits several dipyridyl ring modes at 1604, 1291, and 1234 cm^{-1} which are not present in the spectrum when L = dmb. In addition, femtosecond pump–probe spectroscopy performed at 400 nm yields a transient bleach of the IT absorption band with a single exponential decay of 3.5 ps for L = bpy, compared with only 1.8 ps for L = dmb and 2.1 ps for $[(NC)_5Fe^{II}$-CN-$Pt^{IV}(NH_3)_4$-NC-$Fe^{II}(CN)_5]^{4-}$. Last, prolonged irradiation of the complexes at 488 nm leads to the formation of 4 equiv of ferricyanide with a quantum efficiency of 0.0014 for L = bpy and 0.0011 for L = dmb. The transient absorption, resonance Raman, and photochemical data suggest that the degree of excited electronic coupling in these compounds is tunable by changing the electronic nature of the Pt-L-Pt bridging ligand.

Introduction

Over the past several decades, there has been considerable interest in the design of supramolecular systems that can undergo photoinduced electron transfer following the absorption of a photon of visible light.[1] Mixed-valence (MV) compounds have proven to be particularly useful in this regard.[2] Typically, these species consist of two transition metal complexes (one which serves as an electron donor and the other as an electron acceptor) that are linked to each other by a short ligand bridge. The electronic interaction between the donor−acceptor pair manifests itself in the UV/VIS/near-IR spectrum of the molecule as an intervalent (IT) transition.[3] When the molecule absorbs light having the same frequency as the IT band, an electron is transferred from the donor to the acceptor metal center. Because of the directional nature of the photoinduced electron transfer, MV compounds have potential applications as electrochromic displays, molecular rectifiers, nanoscale switches, and photoinduced magnetic memory devices.[4]

From a theoretical point of view, the kinetic barrier to intramolecular electron transfer can be obtained from the compound's ground-state properties by employing a semiclassical approach, where the rate constant for electron transfer depends on three factors: the thermodynamic driving force, the reorganization energy, and the degree of electronic coupling.[5] The first of these, the thermodynamic driving force, or ground-state free energy difference, can be obtained

* To whom correspondence should be addressed. E-mail: bwpfennig@yahoo.com.

(1) (a) Barbara, P. F.; Meyer, T. J.; Ratner, M. A. *J. Phys. Chem.* **1996**, *100*, 13148. (b) Fox, M. A.; Chanon, M., Eds. *Photoinduced Electron Transfer*; Elsevier: Amsterdam, The Netherlands, 1988. (c) Balzani, V.; Scandola, F. *Supramolecular Photochemistry*; Horwood: Chichester, U.K., 1991.

(2) (a) Creutz, C. *Prog. Inorg. Chem.* **1989**, *30*, 1 and references therein. (b) Vogler, A.; Osman, A. H.; Kunkely, H. *Coord. Chem. Rev.* **1985**, *64*, 159.

(3) Meyer, T. J. *Acc. Chem. Res.* **1978**, *11*, 94.

(4) Ferretti, A.; Lami, A.; Ondrechen, M. J.; Villani, G. *J. Phys. Chem.* **1995**, *99*, 10484.

10.1021/ic020232u CCC: $22.00 © 2002 American Chemical Society
Published on Web 07/12/2002

from electrochemical measurements. The second, the reorganization energy associated with the differing nuclear and solvent configurations for the donor and acceptor metals, can be obtained as the difference in energy between the IT band maximum and the ground-state free energy difference. Last, the magnitude of the electronic coupling (H_{ab}) can be inferred from the oscillator strength of the IT absorption band, according to eq 1, where $\bar{\nu}_{max}$ is the energy of the IT band

$$H_{ab} = \frac{0.0206(\bar{\nu}_{max}\epsilon_{max}\Delta\bar{\nu}_{1/2})^{1/2}}{g^{1/2}r_{ab}} \quad (1)$$

at its maximum (in cm^{-1}), ϵ_{max} is the molar absorptivity of that band, $\Delta\bar{\nu}_{1/2}$ is its full-width at half-maximum (also in cm^{-1}), g is the degeneracy of the transition, and r_{ab} is the vectorial distance that the electron must transfer between the donor and acceptor centroids (usually taken as the crystallographic distance measured in angstroms). The larger the value of H_{ab}, the more rapid the rate of intramolecular electron transfer.

While the intervalent chemistry of dinuclear MV compounds is fairly well understood, only a few multinuclear MV compounds have been investigated. These species contain more than one donor−acceptor pair and the possibility of multiple electron transfer. In particular, a variety of theoretical questions regarding the sequence of multiple electron transfer events remain unanswered. To address some of these questions, we have previously reported a photoinduced, net two-electron transfer occurring in a series of structurally related, cyano-bridged M(II)-Pt(IV)-M(II) triads.[6] For instance, irradiation of the Fe(II) → Pt(IV) IT transition in $[(NC)_5Fe^{II}\text{-}CN\text{-}Pt^{IV}(NH_3)_4\text{-}NC\text{-}Fe^{II}(CN)_5]^{4-}$, hereafter referred to as Fe(II)-Pt(IV)-Fe(II), leads to the formation of $[Pt^{II}(NH_3)_4]^{2+}$ and 2 equiv of $[Fe^{III}(CN)_6]^{3-}$, a net two-electron process. Considerable evidence suggests that a three-state model is required to describe the net two-electron transfer. Photoinduced electron transfer from Fe(II) → Pt(IV) generates a high-energy Fe(III)-Pt(III)-Fe(II) intermediate. This species then accepts a second electron in a subsequent thermal electron-transfer step to yield the observed photoproducts. The three-state model has proven quite successful in predicting how the quantum efficiency of ferricyanide formation varies as a function of the internal barriers to electron transfer across a series of structurally related congeners.[7] It is also consistent with recent femtosecond measurements of the solvent dependence of the back-electron-transfer dynamics that follow photoexcitation of the IT transition.[8]

The focus of this work is to extend our knowledge of multinuclear cyano-bridged MV compounds beyond the two-electron Fe(II)-Pt(IV)-Fe(II) MV systems mentioned above. To this end, we have designed and synthesized two hexanuclear species, each of which contains two Fe(II)-Pt(IV)-Fe(II) triads linked together at the Pt atoms with a symmetric, organic bridging ligand. The proposed structures of the novel MV systems are shown in Figure 1. The synthesis of these particular compounds allowed us to investigate how the electronic nature of the ligand bridge between the two Pt atoms influenced the molecule's excited-state properties. Theoretical calculations have shown that the degree of electronic coupling between two metal centers that are connected by a substituted dipyridyl bridge should decrease when the two pyridyl rings no longer lie in the same plane, showing a minimum at a torsional angle of 45° for a system of similarly substituted diphenyl bridges studied by McClendon and Helms.[9] Proton NMR studies of the 4,4′-dipyridyl ligand (bpy) have estimated the internal barrier to rotation about the C_4-C_4' bond at 4 kcal/mol.[10] Since the most likely mechanism for through-bridge electron transfer is via $\pi-\pi$ coupling, one way to increase the kinetic barrier to electron transfer is to increase the torsional angle between the pyridyl rings. When 3,3′-dimethyl-4,4′-dipyridyl (dmb) is substituted as the bridging ligand, the steric effect of the two methyl groups precludes the ligand from achieving a coplanar arrangement of the pyridyl rings.[11] Thus, this ligand is typically used as a bridge when one wishes to decouple the electronic interaction of one transition metal complex from the other. We have therefore chosen to investigate the hexanuclear MV compounds bridged by bpy and dmb. The ligand field strengths of the two bridges are comparable, as are the internuclear separations, r_{ab}. As a result, any differing electrochemical or spectroscopic properties between the two MV compounds can be attributed to the disparate degrees of excited-state electronic coupling afforded by the bridging ligands.

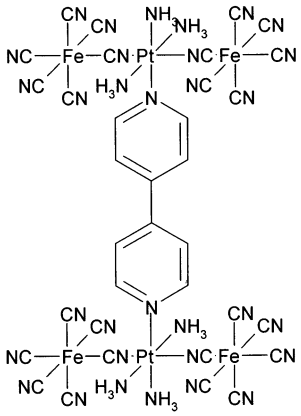

Figure 1. Proposed molecular structures of compound **I** (excluding the cations and waters of hydration). Compound **II** contains methyl groups in the 3,3′-positions of the organic bridging ligand.

(5) (a) Creutz, C.; Newton, M. D.; Sutin, N. *J. Photochem. Photobiol. A: Chem.* **1994**, *82*, 47. (b) Creutz, C. *Prog. Inorg. Chem.* **1989**, *30*, 1. (c) Hush, N. S. *Prog. Inorg. Chem.* **1967**, *8*, 357. (d) Hush, N. S. *Prog. Inorg. Chem.* **1967**, *8*, 391.
(6) (a) Zhou, M.; Pfennig, B. W.; Steiger, J.; Van Engen, D.; Bocarsly, A. B. *Inorg. Chem.* **1990**, *29*, 2456. (b) Pfennig, B. W.; Bocarsly, A. B. *J. Phys. Chem.* **1992**, *96*, 226. (c) Pfennig, B. W.; Bocarsly, A. B. *Comments Inorg. Chem.* **1992**, *13*, 261.
(7) Wu, Y.; Cochran, C.; Bocarsly, A. B. *Inorg. Chim. Acta* **1994**, *226*, 251.
(8) Watson, D. F.; Bocarsly, A. B.; Schreiber, E. Unpublished results.
(9) Launay, J. P.; Woitellier, S.; Sowinska, M.; Tourel, M.; Joachim, C. *Molecular Electronic Devices III*; Elsevier: Amsterdam, The Netherlands, 1988.
(10) Mangutova, Y. S.; Mal'tseva, L. S.; Kamaer, F. G.; Leoutev, B. V.; Mikhamedkhanova, S.; Otroshshenko, O. S.; Sudykov, A. S. *Izv. Akad. Nauk. SSR, Ser. Khim.* **1973**, *7*, 1510.
(11) Gourdon, A. *New J. Chem.* **1992**, *16*, 953.

Experimental Section

Materials. $K_3[Fe(CN)_6]$, trifluoromethanesulfonic acid, and 4,4′-dipyridyl (bpy) were purchased from Sigma-Aldrich, and *trans*-$Pt(NH_3)_2Cl_2$ was either supplied by Strem or synthesized from $[Pt(NH_3)_4]Cl_2$.[12] Bio-Gel P2 polyacrylamide gel was obtained from Bio-Rad. 3,3′-Dimethyl-4,4′-dipyridyl (dmb) was synthesized according to the literature method[13] from β-picoline and chlorotrimethylsilane in THF under an argon blanket, followed by reduction with a 40% mineral dispersion of Na metal in dry THF. Following workup and purification, a yield of 30% was obtained. ^{1}H NMR 300 MHz ($CDCl_3$) 2.64 (s, 6), 7.32 (d, $J = 5$ Hz, 2), 7.38 (s, 2), 8.60 ppm (d, $J = 5$ Hz, 2); MS, *m*/*z* 184, 169, 156, 142, 128, 115. $[Pt(NH_3)_3Cl]Cl$ was synthesized in several steps from *trans*-$Pt(NH_3)_2Cl_2$ according to the literature procedure.[14] The corresponding triflato derivative, $[Pt(NH_3)_3(OSO_2CF_3)](OSO_2CF_3)$, was synthesized by heating a solid sample of $[Pt(NH_3)_3Cl]Cl$ in trifluoromethanesulfonic acid under an argon blanket for 2−3 h at 100 °C, by analogy with the literature procedure for $[Pt(NH_3)_5(OSO_2CF_3)](OSO_2CF_3)_3$.[15]

Synthesis of $[(NH_3)_3Pt-L-Pt(NH_3)_3](OSO_2CF_3)_4$. In a typical procedure, the two $[(NH_3)_3Pt-L-Pt(NH_3)_3](OSO_2CF_3)_4$ species (L = bpy or dmb) were synthesized by the reaction of 0.43 g of $[Pt(NH_3)_3(OSO_2CF_3)](OSO_2CF_3)$ (0.79 mmol, 2 equiv) in 10 mL of deionized H_2O with 1 equiv (0.40 mmol) of the appropriate bridging ligand dissolved in 10 mL of acetone. The resulting mixture was gently heated on a hot plate with stirring for ∼1 h. The solvents were then removed by evaporation and the resulting tan solid was washed with generous portions of diethyl ether and recrystallized from hot deionized H_2O by precipitation with acetone. Yields ranged from 25 to 35%. For L = bpy: ^{1}H NMR 400 MHz (D_2O) 7.75 (d, $J = 6$ Hz, 4), 8.60 ppm (d, $J = 6$ Hz, 4). For L = dmb: ^{1}H NMR 400 MHz (D_2O) 2.60 (s, 3), 3.17 (s, 3), 3.8−4.2 (br, NH_3), 7.59−7.75 (multiplet, 3), 7.90 (d, $J = 25$ Hz, 1), 8.49 (dd, $J = 18$ Hz, $J' = 5$ Hz, 1), 8.96 ppm (dd, $J = 19$ Hz, $J' = 6$ Hz, 1).

Synthesis of I and II. The MV compounds **I** and **II** were synthesized by the aqueous reaction of 4 equiv of $K_3[Fe(CN)_6]$ with 1 equiv of the corresponding $[(NH_3)_3Pt-L-Pt(NH_3)_3](OSO_2CF_3)_4$ species (L = bpy for **I**, L = dmb for **II**). This procedure was analogous to that for the corresponding trinuclear analogue, Fe(II)−Pt(IV)−Fe(II). In a typical synthesis, 0.19 g (0.15 mmol, 1 equiv) of $[(NH_3)_3Pt-L-Pt(NH_3)_3](OSO_2CF_3)_4$ was dissolved in 10 mL of deionized H_2O. To this solution was added 10 mL of an aqueous solution containing 0.20 g (0.60 mmol, 4 equiv) of $K_3[Fe(CN)_6]$. The mixture was allowed to stir in the dark for >4 h, during which time it developed a deep red color. Following removal of the solvent at room temperature in the dark, the residue was dissolved in a minimum amount of deionized H_2O, filtered to remove any insoluble impurities, and loaded onto a Bio-Gel P2 size exclusion column, collecting the major band following elution with deionized H_2O. Typical yields after purification varied from 50 to 65%.

Instrumentation. Electronic absorption spectra were obtained in aqueous solution over the range 200−1100 nm by using a Hewlett-Packard 8453 diode array spectrophotometer. Molar extinction coefficients were determined by dissolving a known quantity of the compound in a 25.00-mL volumetric flask, assuming no waters of hydration in the molecular formula, taking serial dilutions of this stock solution such that the absorbance at the λ_{max} was never larger than 0.25, and fitting these data by using the Beer−Lambert law. Job plots[16] were constructed by making 3.00 -mM solutions of the Pt−L−Pt and Fe starting materials, varying the mole fraction of each complex in 0.10-unit increments, and obtaining the absorbance on the red side of the IT band at 450 nm (where neither of the starting materials absorbed).

IR spectra were collected as KBr pellets over the range 4000−400 cm^{-1} with either a Perkin-Elmer 1600 Series FTIR with 2-cm^{-1} resolution or a Nicolet Model 730 FTIR spectrometer with 4-cm^{-1} resolution and averaging 8 scans. ^{1}H NMR spectra were obtained in the appropriate deuterated solvent as the average of 256 scans with either a Unity INOVA-400 MHz or a Varian 300 MHz NMR spectrometer. Mass spectra were obtained by using a Hewlett-Packard model 6890 gas chromatograph coupled to a HP 5973 mass spectrometer. Cyclic voltammograms were obtained in 1.0 M $NaNO_3$ supporting electrolyte by using a Princeton Applied Research (PAR) 173 potentiostat with a PAR 175 universal programmer, a Houston Instruments XY recorder, and a standard three-electrode configuration (Pt/Pt/SCE).

The quantum efficiency was determined at 488 nm by irradiating 1-mL samples (0.15 mM) with a Coherent Innova 70 argon-ion laser for 3-min intervals from 0 to 18 min at a beam-expanded power of 130 mW/cm^2 and obtaining UV/vis spectra at each interval. The data were fit by using the molar absorptivities measured at 422 and 488 nm for the MV compounds and the ferricyanide ion (970 and 0 M^{-1} cm^{-1}, respectively). The incident laser light intensity was measured by using a calibrated Newport Research model 815 power meter.

Elemental analysis of cyanometalates by commercial laboratories is often difficult to obtain accurately due to the formation of metal carbides. To obtain reliable analyses, a suitable catalyst must be employed. The presence of multiple transition metals adds a further complication. Therefore, the Fe:Pt ratios in compounds **I** and **II** were measured directly by electron microprobe analysis (EPMA) and inductively coupled plasma (ICP). EPMA was performed with a CAMECA SX-50 instrument at the Princeton Materials Institute. This technique focuses a beam of electrons at a micron-sized area of the solid sample, exciting the inner-shell electrons of the material. Upon relaxation back to the ground state, X-ray emission occurs which is characteristic of the elements present.[17] Analyses were performed by using an accelerating voltage of 15 kV and a regulated beam current of 20 nA. The instrument was calibrated by first running a series of commercially available standards for the two metals to be analyzed. $Na_4[(NC)_5Fe^{II}$-CN-$Pt^{IV}(NH_3)_4$-NC-$Fe^{II}(CN)_5]$ was also used as a standard. The results were reported as the average Fe/Pt ratio over 5−10 areas of the bulk sample. The ICP samples were prepared by dissolving the complexes in deionized H_2O to make approximately 90 μM solutions. Analyses were performed on a Perkin-Elmer Optima 4300 DV optical emission spectrometer.

Resonance Raman spectra were obtained in an aqueous solution (1.0 mM) containing 0.5 M potassium sulfate as an internal standard. Due to the known photochemistry of the complexes, Raman spectra were collected with use of a continuous flow jet apparatus. Spectra were recorded in a 135° backscattering geometry with a Spex 1401 triple monochromator equipped with a Hamamatsu R1220 photomultiplier tube and photon counting detection. Laser excitation at 488 nm was obtained from a Spectra Physics model 370 argon ion laser at incident irradiations of 40−50 mW. Off-

(12) Kauffman, G. B. *Inorg. Synth.* **1963**, *7*, 242.
(13) Rebek, J., Jr.; Costello, T.; Wattley, R. *J. Am. Chem. Soc.* **1985**, *107*, 7487.
(14) Morita, H.; Bailar, J. C., Jr. *Inorg. Synth.* **1984**, *22*, 124.
(15) Curtis, N. J.; Lawrance, G. A.; Sargeson, A. M. *Inorg. Synth.* **1986**, *24*, 277.
(16) Vosburgh, W. C.; Cooper, G. R. *J. Am. Chem. Soc.* **1941**, *63*, 437.
(17) Goldstein, J. I. *Scanning Electron Microscopy and X-ray Microanalysis: A Text for Biologists, Materials Scientists, and Geologists*, 2nd ed.; Plenum Press: New York, 1992.

resonance spectra at 647 nm were obtained from a Coherent Innova 100K3 krypton ion laser at an incident power of 90 mW. Both high- (1200−2200 cm^{-1}) and low-frequency (350−1000 cm^{-1}) windows were recorded, using d_6-dmso and dmf as standards for the calibration of the spectra. The data were analyzed with the Galactic GRAMS software package.

Femtosecond transient absorption decay measurements were performed as follows. Approximately 100-fs pulses (7 μJ, 86 MHz repetition rate) of 800-nm light were generated by a Spectra-Physics Tsunami Ti:sapphire oscillator pumped by a Spectra-Physics Millenia 4.5 W Nd:YVO_4 laser. The resulting pulses were sent through a Spectra-Physics Spitfire regenerative amplifier pumped by two Spectra-Physics Merlin Nd:YAG lasers outputting 527-nm light at 13 W. The result was 800-nm pulses of approximately 2 mJ, with a 100-fs pulse width at 1 kHz repetition rate. The 800-nm light from the regenerative amplifier was then converted into 400 nm by passing it through a β-BBO frequency doubling crystal. The 400-nm pulses were attenuated and split 50:50 into pump and probe beams. The probe beam was chopped at 100 Hz, attenuated, and sent through a computer-controlled Physik Instrumente C844-40 translation stage. The parallel pump (400 nm, 100 μJ) and probe (400 nm, <1 μJ) beams were focused onto a 1-cm flow-cell cuvette that contained a continuously flowing aqueous solution of the sample ($A_{400\ nm} \sim 0.8$). After the sample, the pump beam was blocked, and the probe beam was detected with a ThorLabs DET 210 silicon photodiode. The oscillatory component of the probe signal was detected with a Princeton Applied Research model 5208 lock-in amplifier that was output to a Hewlett-Packard 34401A multimeter. The delay stage and multimeter output were controlled and recorded, respectively, by use of National Instruments Labview 5.1 software. Data were acquired in step sizes of 50−100 fs. Raw data were recorded in transmittance mode and were smoothed by averaging three adjacent points. The resulting excited-state lifetimes were obtained by fitting a single exponential to the transmission decay.

Results and Discussion

Synthesis and Characterization. The synthesis of the two $[(NH_3)_3Pt\text{-}L\text{-}Pt(NH_3)_3](OSO_2CF_3)_4$ species (L = bpy or dmb) precursors occurs by a simple substitution reaction of the bridging ligand for triflate in a 2:1 Pt:L ratio. It is well-known that the triflate ion is labile in aqueous solution and that coordination compounds containing this ligand as a leaving group will rapidly react with σ-donating nitrogen ligands.[18] The ^{1}H NMR spectrum of $[(NH_3)_3Pt\text{-bpy-}Pt(NH_3)_3](OSO_2CF_3)_4$ exhibits two downfield doublets, both of which have somewhat larger chemical shifts than those for bpy alone. This indicates that the ligand is indeed bridging the two Pt centers in a symmetric fashion. Furthermore, the IR spectrum of this compound exhibits strong ν_a (NH) and ν_s (NH) stretches at 3263 and 3117 cm^{-1}, δ_a (NH_3) and δ_s(NH_3) bending modes at 1605 and 1387 cm^{-1}, a rocking $\rho(NH_3)$ mode at 928 cm^{-1}, and ν(PtN) stretches at 579 and 517 cm^{-1}, consistent with the Pt(II) oxidation state.[19] A number of weaker ν(CH) stretches and skeletal modes corresponding to the bpy bridge are also observed, as are three strong bands at 1249, 1166, and 1030 cm^{-1}, which can be attributed to the triflate anion.

Table 1. Spectroscopic and Electrochemical Properties of Four MV Compounds Containing the Fe(II)-Pt(IV) Donor−Acceptor Pair

compd	IT λ_{max} (nm)	ϵ_{max} ($M^{-1}\,cm^{-1}$)	fwhm (cm^{-1})	ν(CN) (cm^{-1})	E^o_{Fe} (V vs SCE)
Fe(II)−Pt(IV)	423	1000	7400	2118, 2054	0.56
Fe(II)−Pt(IV)−Fe(II)	424	2360	7200	2125, 2055	0.55
I	421	4230	7400	2122, 2053	0.53
II	421	4240	7600	2118, 2051	0.55

The ^{1}H NMR spectrum of $[(NH_3)_3Pt\text{-dmb-}Pt(NH_3)_3](OSO_2CF_3)_4$ exhibits two upfield singlets, corresponding to two nonequivalent methyl groups on the dmb ligand bridge, as well as a broad peak around 4 ppm, which can be attributed to the ammine ligands on the two Pt centers being hydrogen bonded to the solvent. The downfield region of the spectrum exhibits four doublets of doublets and two additional doublets, whose energies and splitting patterns can be assigned to the six aromatic hydrogens on dmb. The nonequivalence of these hydrogens, as well as those of the two methyl groups, indicates that the two pyridyl rings on the dmb bridge are not coplanar and cannot freely rotate on the NMR time scale. This observation is an important consequence of the steric interaction between methyl groups on the dmb ligand bridge. The IR spectrum of this compound also exhibits strong ν_a(NH) and ν_s(NH) stretches at 3317 and 3225 cm^{-1}, $\delta_a(NH_3)$ and $\delta_s(NH_3)$ bending modes at 1604 and 1344 cm^{-1}, a rocking $\rho(NH_3)$ mode at 858 cm^{-1}, and ν(PtN) stretches at 579 and 520 cm^{-1}, consistent with the Pt(II) oxidation state.[19] A number of weaker ν(CH) stretches and skeletal modes corresponding to the dmb bridge are also observed, as are three strong bands at 1243, 1178, and 1034 cm^{-1}, which can be attributed to the triflate anion.

The syntheses of the MV compounds **I** and **II** are believed to occur by a net four-electron inner-sphere oxidation of the $[(NH_3)_3Pt\text{-L-}Pt(NH_3)_3](OSO_2CF_3)_4$ precursors by four ferricyanide ions, by analogy with the reaction mechanism for $[(NC)_5Fe^{II}\text{-CN-}Pt^{IV}(NH_3)_4\text{-NC-}Fe^{II}(CN)_5]^{4-}$ and its related congeners.[6] Both compounds exhibit two broad peaks in their UV/vis spectra around 315 and 420 nm, having the energies, molar absorptivities, and full-widths at half-maximum (fwhm) listed in Table 1 and giving the complexes a deep blood red color. The lower energy band is assigned as an IT transition from Fe(II) → Pt(IV), by analogy with other cyano-bridged Fe(II)-Pt(IV) species,[6,20] two of which are also listed in Table 1. The molar absorptivities for the IT bands in **I** and **II** are roughly comparable and are approximately twice that for the corresponding Fe(II)-Pt(IV)-Fe(II) triad and four times that of the $[(NC)_5Fe^{II}\text{-CN-}Pt^{IV}(NH_3)_5]$ dyad, hereafter referred to as Fe(II)-Pt(IV). This suggests the additive nature of the Fe(II)-Pt(IV) IT oscillator in these multinuclear complexes and supports the proposed molecular structures of the two compounds. Further evidence for the 4:1 Fe:Pt-L-Pt ratio is supplied by the Job plots of these two species at 450 nm, where only the IT band absorbs. The maximum absorbance at 450 nm for a series of equilibrated samples in which the overall concentration is held constant as the mole fraction of the starting reagents is varied in 0.1 increments from 0.0

(18) Burewicz, A.; Haim, A. *Inorg. Chem.* **1988**, *27*, 1611.
(19) Nakamoto, K. *Infrared and Raman Spectra of Inorganic and Coordination Compounds*, 4th ed.; John Wiley & Sons: New York, 1986.
(20) Pfennig, B. W.; Lockard, J. V.; Cohen, J. L.; Watson, D. F.; Ho, D. M.; Bocarsly, A. B. *Inorg. Chem.* **1999**, *38*, 2941.

to 1.0 occurred at a ratio of 4 Fe:1 Pt-L-Pt. The Fe:Pt ratios of bulk samples of the two compounds are also consistent with the proposed molecular formulas: L = bpy (Fe/Pt = 1.8 by ICP and 1.9 by EPMA), L = dmb (Fe/Pt = 1.9 by ICP and 1.8 by EPMA).

The IR spectrum of **I** contains broad absorptions at 3450, 3210, and 3075 cm^{-1} in the ν(NH) stretching region, strong absorptions at 1617 and 1398 cm^{-1} for the ammine bending modes $\delta(NH_3)$, and rocking modes $\rho(NH_3)$ at 1094 and 969 cm^{-1}, indicating the presence of Pt(IV) ammines in the complex of interest.[19] Strong ν(CN) modes appear at 2122 and 2053 cm^{-1}, consistent with bridging and terminal CN stretches and an Fe(II) oxidation state. Bridging CN stretches typically occur at higher frequencies than those for terminal cyanides as a result of kinematic coupling and shifts of 50−70 cm^{-1} have been observed for similar cyano-bridged species.[21] The presence of bridging cyanides in the IR, as well as the observed Fe(II) oxidation state, adds further support that the complex forms by an inner-sphere electron transfer. Weaker skeletal modes for the bridging ligand are also observed. The low-frequency region of the spectrum contained a multitude of overlapping peaks, corresponding to the various Fe−C and Pt−N stretches present in **I**. Compound **II** exhibits a similar IR spectrum, with peaks at 3434, 3235, 3031, 2118, 2051, 1617, 1384, 1111, and 975 cm^{-1}.

Redox Chemistry. Cyclic voltammograms of **I** and **II** taken in 1 M $NaNO_3$ supporting electrolyte by using Pt working and counter electrodes and a SCE reference yield a single redox event corresponding to the Fe moiety. This potential is shifted several hundred millivolts positive of that for the ferri/ferrocyanide couple[22] as a result of the withdrawing nature of the Pt(IV) species attached to one of the cyanide ligands. Similar shifts in the Fe redox potential have been observed for other cyano-bridged MV compounds. A scan-rate dependence over the range of 10−300 mV/s indicates that this redox process is quasireversible, a result that is also consistent with that for analogous compounds.[6,20,21] The ferri/ferrocyanide couple, for example, is quasireversible in the pH 5−7 range. The presence of a single Fe redox event for the complexes provides strong evidence that the four Fe sites are not in direct electronic communication with each other in the ground state, a result that was also observed for Fe centers in the Fe(II)-Pt(IV)-Fe(II) triad.[6]

The less positive redox potential for **I** implies that the Pt(IV) species is withdrawing slightly less electron density in this complex than in Fe(II)-Pt(IV), Fe(II)-Pt(IV)-Fe(II), or **II**. One possible explanation for this is that the two Pt(IV) centers are in electronic communication with each other through the bridging bpy ligand. If this is the case, the redox potential of the Pt moieties in the Pt-L-Pt unit would be stabilized with respect to **II**, and this stabilization would decrease the degree of electron withdrawal from the Fe(II) center. By contrast, the Fe redox potential remains unaffected for **II** with respect to the dyad and triad model compounds. The absence of a Pt redox event is consistent with model compounds. This result is due to the fact that the Pt(IV)/Pt(II) couple is kinetically slow as a result of the large reorganization energy associated with the geometric change from octahedral to square planar.

Photophysics and Photochemistry. Irradiation of the IT bands for **I** and **II** at 488 nm leads to the following changes as a function of time in the UV/vis spectra of these complexes: (a) the IT band diminishes; (b) the position of the lowest energy transition shifts from 421 to 416 nm, where the LMCT band of ferricyanide is known to absorb;[23] and (c) a new set of peaks centered around 300 nm begins to appear, which can also be attributed to the formation of ferricyanide. By analogy with the related Fe(II)-Pt(IV)-Fe(II) triad,[6] these results can be interpreted as the gradual loss of Fe(II)-Pt(IV) oscillators and the concomitant formation of ferricyanide. It has been previously established that the photochemistry of Fe(II)-Pt(IV)-Fe(II) leads to a net two-electron process yielding two ferricyanides and one $[Pt(NH_3)_4]^{2+}$. Cyclic voltammetry of the photolysis mixtures confirms the presence of the ferricyanide photoproduct, having a redox potential of 0.2 V vs SCE. Following exhaustive irradiation, both hexanuclear complexes completely lose their IT bands and the resulting absorption spectrum closely resembles that of the ferricyanide ion. The quantum efficiency of ferricyanide formation for each of the novel MV compounds was calculated by fitting the absorbances at 421 and 488 nm over 3-min intervals to those predicted based on the molar absorptivities of the IT bands and ferricyanide at these wavelengths and by using a least-squares analysis of the data. Assuming that the total number of equivalents of ferricyanide formed per photon absorbed is four,[24] the quantum efficiency of ferricyanide formation was 0.0014 for **I** and 0.0011 for **II**. Both of these quantum efficiencies are an order of magnitude smaller than that for Fe(II)-Pt(IV)-Fe(II).[6] In the latter species, the one-electron Fe(III)-Pt(III)-Fe(II)* excited state is followed by a thermal intramolecular electron transfer to yield the observed photoproducts. In the hexanuclear species, a total of four electrons must be transferred to achieve the observed products. If one assumes that electron transfer across the Pt-L-Pt bridge is slower than electron transfer between the cyano-bridged Fe and Pt, the smaller quantum efficiencies for the hexanuclear MV compounds are expected. Indeed, the slightly larger quantum efficiency for **I** than for **II** might imply that electron transfer across the Pt-L-Pt bridge is more rapid in the former case, a result that is consistent with the resonance Raman and time-resolved spectroscopy reported below.

Resonance Raman Spectroscopy. The resonance Raman spectra for **I** and **II** with 488-nm irradiation are shown in

(21) Bignozzi, C. A.; Argazzi, R.; Schoonover, J. R.; Gordon, K. C.; Dyer, R. B.; Scandola, F. *Inorg. Chem.* **1992**, *31*, 5260.
(22) Curtis, J. F.; Meyer, T. J. *Inorg. Chem.* **1982**, *21*, 1562.
(23) Lever, A. B. P. *Inorganic Electronic Spectroscopy*; Elsevier: New York, 1984.
(24) One reviewer has argued, quite correctly, that it is difficult to prove whether one photon initiates a net four-electron transfer in these MV compounds. Since the IT band energies for the hexanuclear and trinuclear MV species are quite similar, it is also possible that the observed photoproducts are formed by consecutive one-photon, net two-electron transfers from each of the bridged triads.

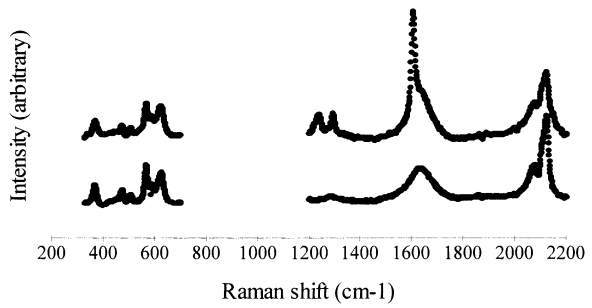

Figure 2. Resonance Raman spectra of **I** (top) and **II** (bottom) with 488 nm irradiation over the ranges 350−700 and 1200−2200 cm^{-1}.

Table 2. Resonance Raman Data (cm^{-1}) for Four MV Compounds Containing the Fe(II)-Pt(IV) Donor−Acceptor Pair, Using 488-nm Irradiation

peak assignment	Fe(II)−Pt(IV)	Fe(II)−Pt(IV)−Fe(II)	**I**	**II**
$\nu(CN)_{bridge}$	2126	2125	2121	2121
$\nu(CN)_{terminal}$	2082	2081	2078	2077
bpy ring str (**8a**)			1604	
bpy inter-ring str Ω			1291	
bpy CH ip bend (**9a**)			1234	
$\nu(FeC)_{axial}$	627	623	623	623
$\nu(FeC)_{radial}$	588	587	586	586
$\nu(FeC)_{bridge}$	570	566	565	565
$\nu(PtN)_{in\ phase}$	508	506	505	504
$\nu(PtN)_{out\ of\ phase}$	475	472	471	472
δ(FeCN)	426	422		
ν(PtNC)	368	366	367	367

Figure 2 over the ranges of 350−700 and 1200−2200 cm^{-1}. A list of the observed peaks for these and related compounds, as well as their tentative assignments, can be found in Table 2.[20,25] For the most part, the energies and relative intensities of the resonantly enhanced vibrational modes are remarkably similar for all four compounds. Bridging, axial, and radial ν(CN) stretches dominate the high-frequency range (2000−2200 cm^{-1}), while numerous metal ligand modes occur in the low-frequency regime (300−700 cm^{-1}). Off-resonance experiments performed on **I** and **II** at 647 nm have shown that the broad band observed in both of these complexes around 1640 cm^{-1} is present in a 0.5 M aqueous solution of K_2SO_4 alone and is therefore artifactual. Furthermore, none of the peaks listed in Table 2 were observed in the off-resonance Raman spectra. This would indicate that all of the vibrational modes listed in Table 2 contribute to the inner-sphere reorganization term for the photoinduced electron transfer, since only those modes that are affected by IT irradiation will be resonantly enhanced.

The one notable difference between the four spectra occurs in the middle of the Raman spectrum in the range of 1200−1650 cm^{-1}. In this region, compound **I** exhibits a strong Raman band at 1604 cm^{-1} and two weaker bands at 1291 and 1234 cm^{-1}, which are absent entirely from any of the other three MV compounds. These bands have been assigned to bpy bridging ligand ring modes. Adapting the Wilson notation[26] for benzene, the 1604 cm^{-1} is assigned as ring stretch (**8a**), while the 1291 and 1234 cm^{-1} modes correspond with the inter-ring stretch Ω and the CH in-plane bend (**9a**), respectively. Similar bands have been observed in the MLCT transitions of bpy-bridged organometallic species. For example, $[(CO)_5W(bpy)W(CO)_5]$ exhibits bands at 1613, 1301, and 1228 cm^{-1} that are attributable to corresponding modes of the bpy-bridging ligand,[27] while these same modes are observed in $[L(CO)_3Re(bpy)Re(CO)_3L]^{2+}$ (L = 4,4′-dimethyl-2,2′-dipyridyl) at 1621, 1301, and 1233 cm^{-1}.[28] In both complexes, irradiation was initiated into a metal-to-bridging bpy ligand charge-transfer excited state. Resonantly enhanced MLCT bpy modes were also observed in $[Ru(NH_3)_5bpy]^{2+}$ at 1603, 1300, and 1230 cm^{-1}.[29]

These data provide strong evidence that IT band irradiation of **I** at 488 nm creates a nuclear distortion that partially involves the bpy bridging ligand. In other words, the observed ring modes of the bpy ligand contribute to the inner-sphere reorganization energy for photoinduced ET in **I**. This result implies that the excited electron in this MV species does not remain localized on a single Pt center, but is partially delocalized onto the bpy bridge. Furthermore, the absence of any ring modes for the dmb bridging ligand in **II** suggests that the MO populated by IT band irradiation in this species does not contain a significant degree of bridging ligand character. While resonant enhancement of bridging ligand modes could also occur if the IT irradiation overlapped with a remote MLCT transition from Fe(II) → L, there was no evidence for remote MLCT bands in the electronic spectra of these complexes (the IT bandwidths and energies were comparable to those for model compounds), and the energies of such bands should not differ significantly between the two compounds.

Since the irradiation of the Fe(II) → Pt(IV) IT band can only effect a single electron transfer, the one-electron localized excited state is best described as {Fe(II),Fe(III)}-Pt(III)-L-Pt(IV)-{Fe(II),Fe(II)}*. The difference between the two Raman spectra, however, indicates that the excited electron in **I** affects several of the vibrational modes on the remote bpy ligand bridge. Given the fact that the ligand field strengths and internuclear separations for the two ligand bridges are comparable, the most plausible explanation for the different resonance Raman results is that the electronic nature of the bpy bridge in **I** allows for an observable degree of excited state electronic coupling between the two Pt atoms, while the twisted ring structure of the dmb bridge significantly prevents this coupling in **II**. This result is illustrated in Figure 3, where the initial IT excitation in **II** is localized on a single Pt atom, while the intervalent excited state of **I** involves the entire Pt-L-Pt bridge. The control of the degree of electronic coupling between adjacent metal centers by varying the electronic nature of the ligand bridge from bpy to dmb has been observed previously in the excited state properties of ligand-bridged compounds following MLCT irradiation. To the best of our knowledge, however, this is the first example of excited-state electronic coupling fol-

(25) Pfennig, B. W.; Wu, Y.; Kumble, R.; Spiro, T. G.; Bocarsly, A. B. *J. Phys. Chem.* **1996**, *100*, 5745.
(26) Wilson, E. B. *Phys. Rev.* **1934**, *45*, 706.
(27) McNicholl, R.-A.; McGarvey, J. J.; Al-Obaidi, A. H. R.; Bell, S. E. J.; Jayaweera, P. M.; Coates, C. G. *J. Phys. Chem.* **1995**, *99*, 12268.
(28) Omberg, K. M.; Schoonover, J. R.; Meyer, T. J. *J. Phys. Chem.* **1997**, *101*, 9531.
(29) Caswell, D. S.; Spiro, T. G. *Inorg. Chem.* **1987**, *26*, 18.

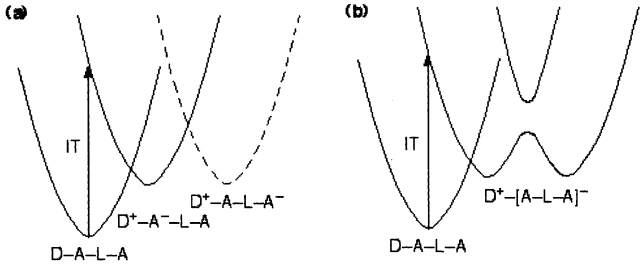

Figure 3. (a) Proposed potential energy diagram for the states involved in the Fe(II) → Pt(IV) IT irradiation of **II**, where localized Fe(III)-Pt(III)-Pt(IV)* oxidation states are implied in the one-electron excited state. (b) Proposed potential energy diagram for the states involved in the Fe(II) → Pt(IV) IT irradiation of **I**, where the excited electron is partially delocalized across the Pt-L-Pt bridge. For clarity, only those metals involved in the IT transition and its corresponding one-electron excited state are shown. Abbreviations: D = donor metal (Fe), L = bridging ligand, A = acceptor metal (Pt), IT = IT absorption band.

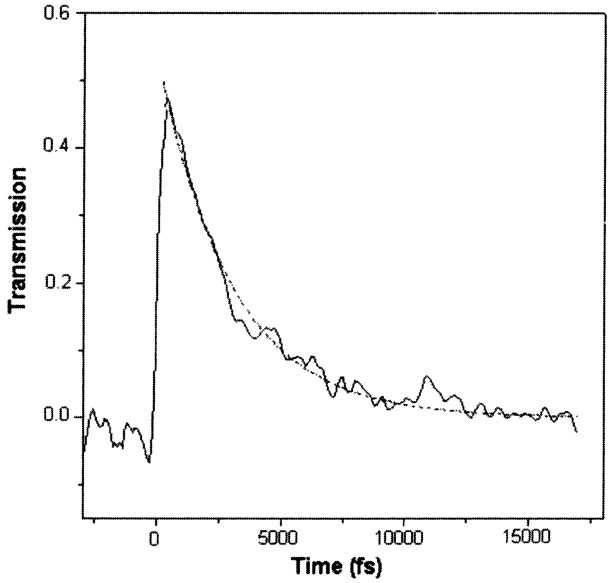

Figure 4. Smoothed femtosecond transient transmission data for **I** with 400 nm pump and probe wavelengths. The dashed line is a single-exponential fit to the experimental data, yielding an excited-state lifetime of 3.2 ps.

lowing IT irradiation. In this scenario, IT irradiation does not necessarily lead to an unstable Pt(III) excited state, since the electron can be delocalized onto the ligand bridge. Excited-state electron transfer across the molecule can then occur by analogy to the "chemical mechanism" for inner-sphere electron transfer.[30]

Femtosecond Pump−Probe Spectroscopy. Single-color pump−probe experiments (400 nm) were performed on the hexanuclear MV compounds, as well as on the model compound Fe(II)-Pt(IV)-Fe(II), in an effort to determine the lifetime of the intervalent excited state. The change in transmittance of the probe beam as a function of time was recorded. Figure 4 illustrates the bleach of the IT band at 400 nm for **I**. The data were well fit by a single exponential, yielding an excited-state lifetime of 3.2 ps for **I**, 1.8 ps for **II**, and 2.1 ps for Fe(II)-Pt(IV)-Fe(II). The observed excited-state dynamics for Fe(II)-Pt(IV)-Fe(II) are comparable to those reported previously. Likewise, the similar lifetimes for **II** and Fe(II)-Pt(IV)-Fe(II) is not surprising, given that the energy of the IT bands and the redox potentials of the metals in these two complexes are nearly identical. Thus, the back-electron transfer following IT irradiation must occur with a similar rate constant for each species, as predicted by semiclassical electron transfer theory.[5] This result lends further credence to the localized excited state shown in Figure 3a for **II** and suggested by the resonance Raman data. Likewise, the longer excited-state lifetime for **I** is consistent with an excited state where the electron is partially shared by the Pt-L-Pt bridge, as shown in Figure 3b. Partial delocalization of the excited electron onto the bpy bridging ligand effectively increases the distance r_{ab} that the electron has traveled. If this were indeed the case, it would imply a decreased rate constant for the back-electron transfer.

Summary

The intervalent properties of two hexanuclear MV compounds were investigated, where each of the compounds contained two Fe(II)-Pt(IV)-Fe(II) triads linked to each other through a Pt-L-Pt bridge. The electronic nature of the bridging ligand L was tuned by adjusting the substituents on the dipyridyl ring. For L = bpy, the two pyridyl rings could rotate freely and π-conjugation could occur across the ligand bridge as the torsional angle approached zero. On the other hand, for L = dmb, steric hindrance of the methyl groups forced the two pyridyl rings into a noncoplanar arrangement that decreased the degree of overlap between π-orbitals on the two halves of the ligand. When these two bridging ligands were incorporated into the hexanuclear MV compounds, several differences were observed in the electronic properties of these species that could be interpreted as resulting from the differing degrees of electronic coupling across the Pt-L-Pt bridges in the intervalent excited state. The most significant difference between the two MV compounds was the observation of bpy ring modes in the resonance Raman spectrum of **I** in a region where no comparable dmb modes were observed for **II**. This result provided evidence that the excited electron in the former species is partially delocalized onto the bpy ligand bridge. The longer excited-state lifetime of **I** than **II** also supported this hypothesis, since the rate of back-electron transfer is expected to decrease as the separation of charge increases. These results suggest that the excited-state properties of multinuclear MV compounds can be controlled in a systematic way by the choice of the bridging ligand and pave the way for the rational design of multielectron photocatalysts.

Acknowledgment. The authors acknowledge Dr. T. G. Spiro for the use of his resonance Raman equipment and Dr. C. Coyle and E. Schreiber for technical assistance. Acknowledgment is also made to the donors of the Petroleum Research Fund, administered by the American Chemical Society, for their generous support of this research.

IC020232U

(30) Haim, A. *Prog. Inorg. Chem.* **1983**, *30*, 273.